International Journal of Power Electronics and Drive System (IJPEDS)
Vol. 17, No. 4, December 2026, pp. 2440~2456
ISSN: 2088-8694, DOI: 10.11591/ijpeds.v17.i4.pp2440-2456

Modeling and controlling BLDC motor in electric power steering using fractional order PID controller

Amir Haziq Nordin[1], Azrita Alias[1], Auzani Jidin[1], Maaspaliza Azri[1], Tole Sutikno[2,3]
[1]Department of Engineering, Faculty of Electrical Technology and Engineering, Universiti Teknikal Malaysia Melaka, Melaka, Malaysia
[2]Department of Electrical Engineering, Faculty of Industrial Technology, Universitas Ahmad Dahlan, Yogyakarta, Indonesia
[3]Embedded System and Power Electronics Research Group (ESPERG), Yogyakarta, Indonesia

Article Info

Article history:

Received Jul 20, 2026
Revised Aug 26, 2026
Accepted Oct 4, 2026

Keywords:

BLDC motor
Duty cycle
Electric drive
Fractional-order PID
PI control
Pre-filter
Speed control

ABSTRACT

Brushless DC (BLDC) motors are widely used in electric power steering (EPS) systems because of their high efficiency, compact structure, and fast dynamic response. Nevertheless, inverter switching and electronic commutation may introduce speed fluctuations that reduce steering smoothness, making effective speed regulation essential. This paper investigates a closed-loop speed control strategy that combines a fractional-order proportional–integral–derivative (FOPID) controller with a first-order reference low-pass pre-filter for a three-phase BLDC motor. A unified MATLAB/Simulink model incorporating PWM generation, inverter switching, and Hall-sensor commutation was developed to evaluate the proposed approach against a conventional proportional–integral (PI) controller under identical operating conditions. Performance was evaluated using a multi-step reference speed profile (1200–3500–2000 rpm) with a constant load-torque disturbance based on rise time, settling time, overshoot, undershoot, and steady-state error. The results show that the reference low-pass pre-filter eliminates overshoot and produces smoother speed transitions for both controllers. Compared with the PI controller, the FOPID controller provides improved settling behavior and steady-state accuracy during selected operating conditions while maintaining stable speed tracking. Overall, the proposed combination of the FOPID controller and the reference low-pass pre-filter offers a practical solution for improving BLDC motor speed regulation in EPS applications.

This is an open access article under the CC BY-SA license.

Corresponding Author:

Azrita Alias
Department of Engineering, Faculty of Electrical Technology and Engineering
Universiti Teknikal Malaysia Melaka
76100 Hang Tuah Jaya, Melaka, Malaysia
Email: azrita@utem.edu.my

1. INTRODUCTION

Electric power steering (EPS) has become a widely adopted steering-assist technology in modern vehicles because it improves energy efficiency, reduces maintenance requirements, and integrates more easily with advanced driver assistance systems than conventional hydraulic steering systems [1], [2]. The performance of an EPS system depends greatly on the electric motor drive, which must deliver fast and accurate speed regulation under varying steering conditions. Among the available motor technologies, the brushless direct current (BLDC) motor is widely preferred because of its high efficiency, compact size, high torque density, rapid dynamic response, and long service life resulting from the absence of brushes and mechanical commutators [3], [4]. Despite these advantages, BLDC motors remain susceptible to torque ripple and speed

fluctuations caused by electronic commutation and inverter switching. These effects become more pronounced during rapid speed changes and load disturbances, potentially reducing steering smoothness and overall driving performance [5]–[7].

Improving the speed regulation of BLDC motors has been a focus of numerous research efforts over the last decades. Because of their simplicity, convenient setup, and reliable operation, PI and PID controllers are currently the most widely used controllers [8]–[11]. However, when the control parameters are fixed, they are typically unable to provide satisfactory dynamic performance in a nonlinear or parameter-changing (or even external environment) situation. A variety of advanced control methods are now being developed to address these limitations, such as intelligent control, adaptive control, model predictive control, and fractional-order control, in a bid to improve the transient response, robustness, and tracking performance of BLDC motor drives, and other control methods are still being explored today. For example, a sensorless BLDC motor control method based on back-EMF zero-crossing detection using line voltage differences was proposed to determine rotor position information for electronic commutation [12]. In addition, Zawawi *et al.* [13] demonstrated better dynamic torque control in inverter-fed motor drives by a modified stator flux control strategy, while Wong and Holliday [14] improved low-speed direct torque control performance in induction motors by rotating the switching sectors to minimize stator flux droop. These studies also demonstrate the ongoing quest for improving the dynamic performance, robustness, and efficiency of electric motor drives.

However, only limited attention has been devoted to the combination of fractional-order speed control with reference signal conditioning for BLDC motors in electric power steering applications. Of these advanced control approaches, the FOPID controller has been widely adopted as it extends the conventional PID controller by introducing two additional tuning parameters: the fractional integral order λ and fractional derivative order μ. This additional degree of freedom in control of the controller has been shown to enhance transient response, disturbance rejection, and robustness of the controller compared to the traditional integer-order control [15]. Sharma *et al.* [16] demonstrated that a FOPID controller implemented with the FOMCON toolbox achieved superior transient response and speed tracking performance compared to a conventional PID controller for BLDC motor speed control. In addition, George *et al.* [17] proposed an optimized FOPID controller that further augmented the dynamic nature of BLDC motor drives through controller parameter optimization. These studies confirm the effectiveness of fractional-order control for improving BLDC motor performance. However, their primary focus is on controller design and parameter optimization, and only limited attention has been paid to improving the quality of the reference signal applied to the controller.

Besides controller design, reference signal conditioning has also been recognized as an effective approach for improving transient performance. A first-order reference low-pass pre-filter smooths abrupt changes in the speed command before it is processed by the controller, thereby reducing aggressive control action and producing smoother speed transitions. Although filtering techniques have been reported to improve control stability and transient response, they are generally investigated independently of fractional-order controllers. Consequently, the combined application of a FOPID controller with a reference low-pass pre-filter for BLDC motor speed regulation in electric power steering applications remains insufficiently investigated.

Motivated by this research gap, this paper proposes the integration of a fractional-order proportional-integral-derivative (FOPID) controller with a first-order reference low-pass pre-filter for BLDC motor speed control in electric power steering (EPS) applications. A unified MATLAB/Simulink model is developed to evaluate four controller configurations, namely PI, FOPID, PI with a low-pass pre-filter, and FOPID with a low-pass pre-filter, under identical operating conditions. Their performances are compared in terms of rise time, settling time, overshoot, undershoot, and steady-state error to assess the effectiveness of reference pre-filtering in enhancing BLDC motor speed regulation.

2. METHOD

This section presents the proposed BLDC motor speed control methodology, including the BLDC drive system modelling, closed-loop controller design, and the simulation setup and modelling assumptions used for performance evaluation.

2.1. BLDC drive system configuration

A typical BLDC drive consists of a controller, a power conversion stage (inverter), the BLDC motor, and sensor feedback needed for electronic commutation and monitoring [10], [18]. Based on the basic BLDC system configuration, the controller processes the command and sensor feedback, then sends switching signals to the inverter, which supplies the appropriate electrical power to the motor, and position sensors provide feedback to ensure correct operation. Figure 1 shows the overall hardware block diagram used in this project. As indicated in Figure 1, the main hardware elements include the controller board, inverter module, BLDC motor, the feedback signals from the motor, and the host/communication link used for monitoring during testing.

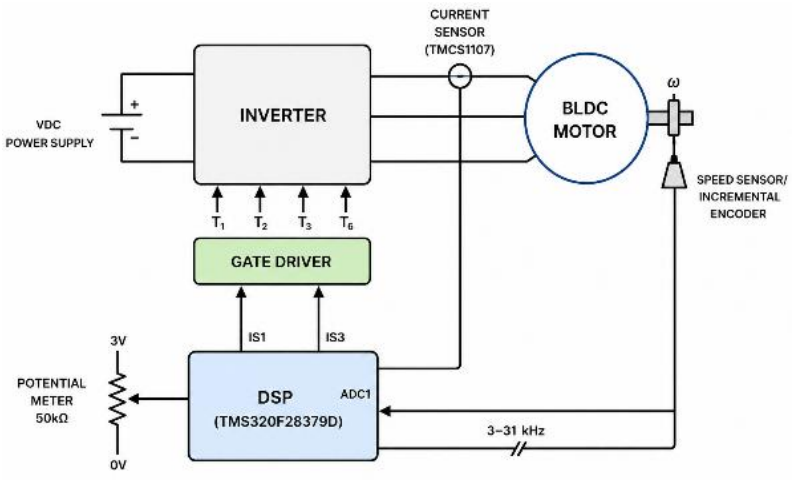

Figure 1. Overall hardware block diagram of the implemented BLDC drive system

The controller generates PWM switching signals for the inverter module, while measured feedback signals are acquired for monitoring and evaluation. The inverter drive module functions as the power stage that interfaces the DC supply and the motor; it converts a fixed DC input into a controlled output through high-frequency switching commanded by the controller PWM signals [19]. The PWM duty ratio is defined as (1).

$$D = \frac{T_{ON}}{T} \tag{1}$$

Where (D) is the duty ratio, (T_{ON}) is the switch ON time, and (T) is the PWM period. As illustrated in Figure 2, increasing duty ratio increases the "ON" duration within each switching period, thereby increasing the average applied voltage.

Under the averaged PWM assumption, the inverter is modelled as a linear gain, where the average output voltage is proportional to the duty cycle and the DC-link voltage, as shown in (2) [20].

$$V_{avg} = DV_{dc} \tag{2}$$

Functionally, the inverter module includes the PWM input interface, gate-driver conditioning, inverter power switches, and the motor terminals, which together establish the signal or power flow from controller to motor. The BLDC motor is equipped with Hall sensors for commutation and an incremental encoder for speed measurement, supporting rotor-position detection and speed monitoring in the overall configuration.

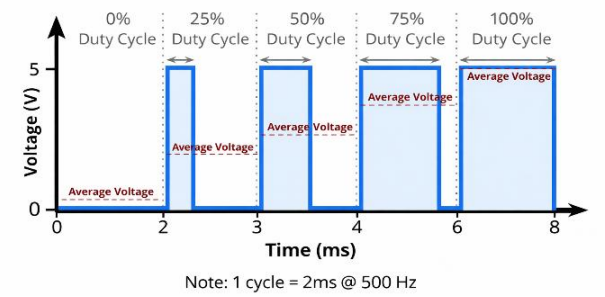

Figure 2. Illustration of PWM duty-cycle variation and its effect on average voltage (0–100% duty cycle)

2.1.1. Hall sensor feedback for electronic commutation

In the BLDC drive configuration, rotor position information is obtained using Hall-effect sensors integrated in the motor [21]. The three Hall signals (H_a, H_b, H_c) provide discrete rotor-position states that are used for electronic commutation. Figure 3 illustrates the Hall-sensor logic control circuit used to generate the inverter gate commands based on the Hall states. The Hall signals are processed through Boolean logic to produce the six switching signals $(S_1 - S_6)$ required for six-step commutation.

Based on Figure 4 and Table 1, the BLDC motor operates using a six-step commutation sequence, where each valid Hall sensor combination (H_a, H_b, H_c) corresponds to a specific commutation sector and inverter switching state (($S_1 - S_6$). During each commutation interval, two MOSFETs are activated to energize two motor phases, while the remaining phase is left floating, ensuring the correct current path for continuous rotor rotation [22].

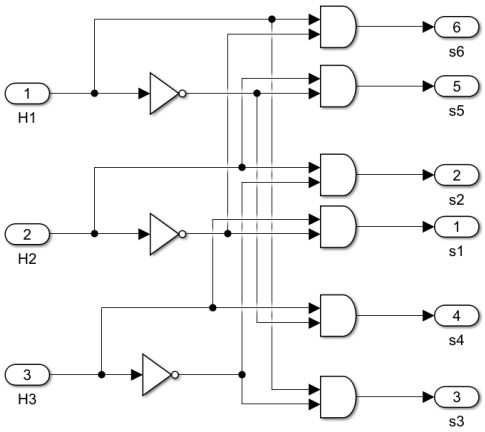

Figure 3. Hall-sensor-based commutation logic control circuit

Table 1. Six-step commutation truth table

Hall sensor signal ($H_a - H_c$)			Switching state for MOSFETs (S1−S6)					
H_a	H_b	H_c	S1	S2	S3	S4	S5	S6
1	1	0	1	0	0	1	0	0
0	1	0	1	0	0	0	0	1
0	1	1	0	0	1	0	0	1
0	0	1	0	1	1	0	0	0
1	0	1	0	1	0	0	1	0
1	0	0	0	0	0	1	1	0

2.1.2. BLDC electrical model (per-phase) and back-EMF relation

As shown in Figure 5, each phase of the BLDC motor can be represented by a series combination of phase resistance, phase inductance, and a back electromotive force (back-EMF) source. The corresponding electrical model for each phase ($k = a, b, c$) is expressed by (3) [23].

$$V_{kn}(t) = i_n R_n + L_n \frac{dik}{dt} t + e_n(t) \quad (3)$$

Where $V_{kn}(t)$ denotes the phase voltage with respect to the neutral point, $i_k(t)$ is the phase current, and $e_k(t)$ represents the phase back electromotive force (back-EMF). The parameters R_k and L_k denote the phase resistance and phase inductance, respectively. In addition to the electrical model, the mechanical dynamics of the BLDC motor must also be considered to accurately describe the rotor motion. The rotational dynamics of the motor are illustrated in Figure 6 and mathematically expressed by (4) [24].

$$T_d(t) = \omega(t)b + J\frac{d\omega}{dt} + T_l(t) \quad (4)$$

Where $T_d(t)$is the developed electromagnetic torque, $\omega(t)$ denotes the rotor angular speed, $b$is the viscous friction coefficient, and $J$is the rotor/load equivalent moment of inertia. The term $T_l(t)$ represents the load torque acting on the motor shaft. The developed electromagnetic torque (T_d) and the back-EMF (e_{phase}) in terms of current and speed, as expressed in (5) and (6), respectively.

$$T_d = k_{t-a} i_a + k_{t-b} i_b + k_{t-c} i_c \quad (5)$$

$$E_k = k_e \omega(t) \quad (6)$$

Where k_e is the back-EMF constant and $\omega(t)$ is the rotor angular speed.

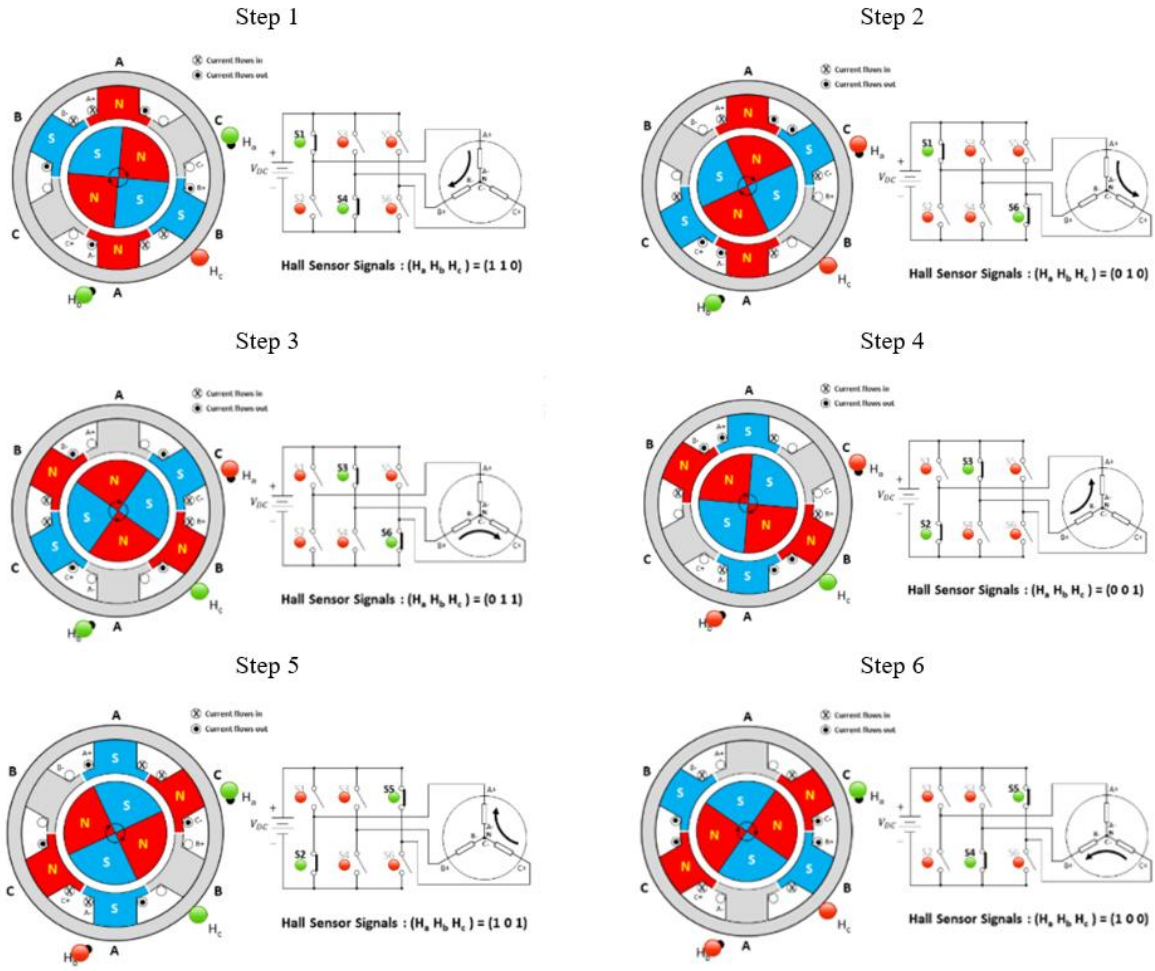

Figure 4. Six-step commutation sequence of BLDC motor

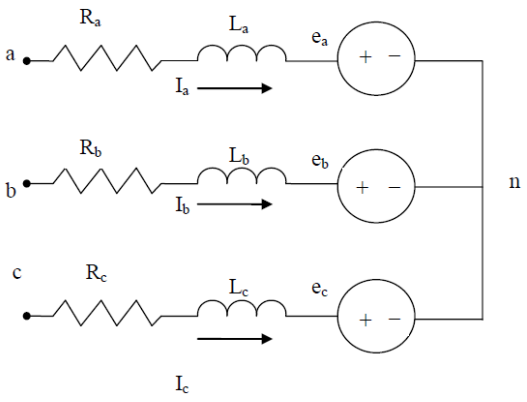

Figure 5. Three-phase BLDC machine equivalent circuit

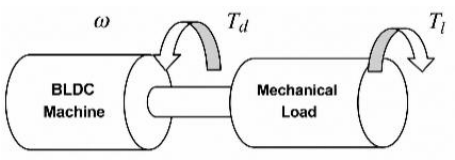

Figure 6. BLDC mechanical coupling

The developed electromagnetic torque depends on the rotor position and phase current, whereas the phase back-EMF depends on the rotor angular position and rotor angular speed [25], [26]. Subsequently, (3)-(6) are transformed into the Laplace domain to establish the relationship between the phase back-EMF, $e_k(t)$, the phase current, $i_k(t)$, the developed electromagnetic torque, $T_d(t)$ and the rotor angular speed, $\omega(t)$, where these equations are then used to construct the block diagram shown in Figure 7. The motor ratings and specifications used in this study are summarized in Table 2.

Table 2. BLDC motor specifications

Parameter	Symbol	Value
Nominal voltage	V_r	36 VDC
No-load speed	n_0	4800 ± 10% rpm
No-load current (max.)	I_0	0.9 A
Rated speed	n_r	4000 ± 10% rpm
Rated torque	T_r	0.48 Nm
Output power	P_r	200 W
Back-EMF constant	K_e	7.5 V/kRPM
Torque constant	K_t	0.072 Nm/A
Phase-to-phase resistance	R_{pp}	0.42 Ω
Number of poles	N_p	4

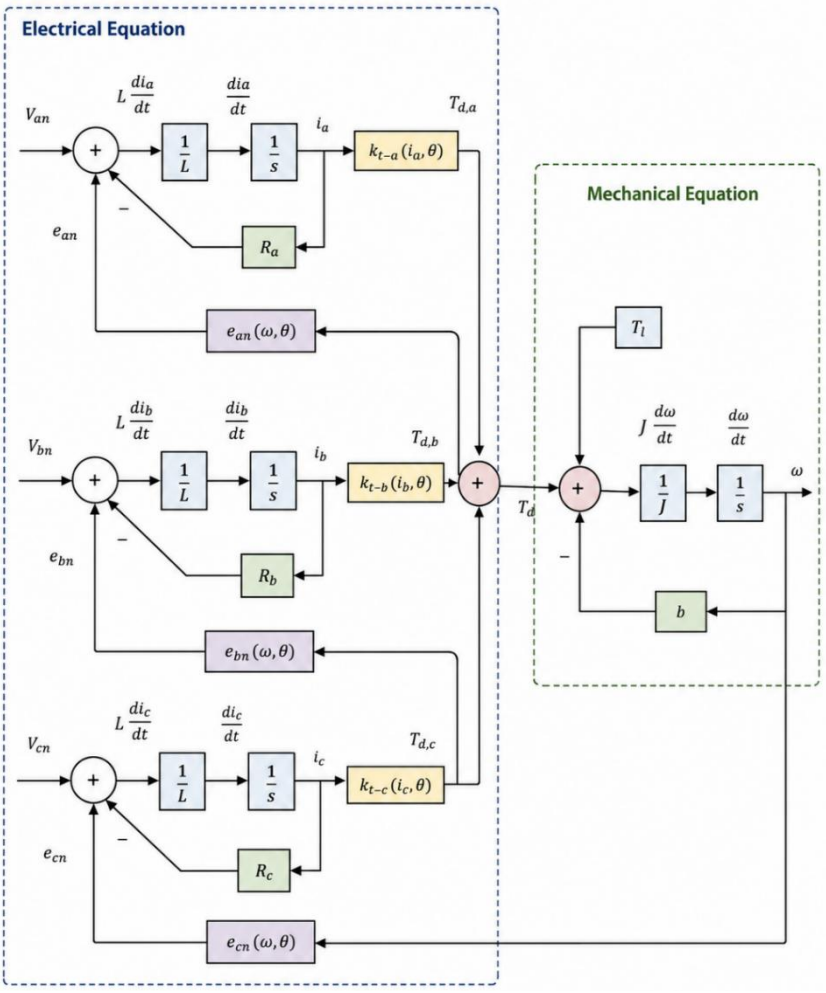

Figure 7. BLDC machine model block diagram

To ensure consistent inverter switching and reliable real-time operation, the PWM gate signals are generated using the enhanced pulse width modulation (ePWM) module, which provides deterministic timing and supports switching-related protection features, including dead-time insertion [27]. The generated PWM

signals are then applied to the inverter drive module to control the switching of the power semiconductor devices at the desired PWM switching frequency.

In the real-time implementation, the controller timing parameters are determined by the sampling period and the PWM switching period. The controller sampling period T_s and PWM switching period T_{PWM} are defined by (7) and (8), respectively [28].

$$T_s = \frac{1}{f_s} \tag{7}$$

$$T_{PWM} = \frac{1}{f_{PWM}} \tag{8}$$

Where f_s is the sampling frequency and f_{PWM} is the PWM switching frequency. Table 3 shows that the overall control execution follows the selected sampling time, while the PWM switching blocks follow the PWM timing configuration.

Table 3. Frequency setup

Parameter	Value
PWM frequency, f_{PWM}	10 kHz
PWM period, T	10 ms
Sampling time	10 ms

2.2. Closed-loop controller design

The closed-loop speed control structure is developed to evaluate the performance of different controllers under identical operating conditions. The controllers are integrated into the BLDC drive simulation model, which includes the inverter, Hall-sensor feedback, and speed measurement. As illustrated in Figure 7, the reference speed $n_{\text{ref}}(t)$ is continuously compared with the measured motor speed $n(t)$ to generate the speed error $e(t)$, which is defined as (9).

$$e(t) = n_{\text{ref}}(t) - n(t) \tag{9}$$

Figure 8 presents the proposed closed-loop speed control structure implemented in the BLDC drive simulation model. The reference speed, $n_{\text{ref}}(t)$ is continuously compared with the measured speed, $n(t)$, to generate the speed error, $e(t)$ which is processed by the controller to produce the duty-cycle command, $u(t)$. The controller output is constrained within the valid PWM duty-cycle range of $0 \leq u(t) \leq 1$ using a saturation block before being applied to the PWM generator, thereby ensuring valid modulation signals and preventing overmodulation. The PWM generator subsequently generates the switching signals required by the power inverter to drive the BLDC motor through the six-step commutation sequence. Rotor position information obtained from the Hall sensors is processed by the timer and speed calculation blocks to estimate the motor speed and synchronize the commutation process. The estimated speed is continuously fed back to the summing junction, forming a closed-loop feedback system that minimizes the speed tracking error and maintains stable motor operation under varying operating conditions

2.3.2. PI controller design and parameter tuning

A proportional–integral (PI) controller is employed to regulate the BLDC motor speed by minimizing the speed tracking error between the reference speed and the measured motor speed. The proportional term provides an immediate corrective action to improve the transient response, while the integral term eliminates the steady-state error by accumulating the speed error over time. Owing to its simple structure, ease of implementation, and satisfactory performance, the PI controller remains one of the most widely adopted control strategies for motor drive applications [8], [23]. The transfer function of the PI controller is expressed as (10), where K_p and K_i denote the proportional and integral gains, respectively.

$$G_{PI}(s) = K_p + \frac{K_i}{s} \tag{10}$$

Figure 9 illustrates the implementation of the PI controller within the proposed closed-loop speed control system. The speed error $e(t)$ is processed through the proportional and integral paths, and the combined controller output is applied to the BLDC motor drive to regulate the motor speed. The PI controller parameters were determined using an iterative simulation-based tuning procedure under the operating conditions described

in section 2.3. The proportional gain K_p was first adjusted to obtain a satisfactory transient response, followed by refinement of the integral gain K_i to eliminate the steady-state error while maintaining system stability and avoiding excessive overshoot. The tuning process was repeated until a satisfactory balance between rise time, settling time, overshoot, and steady-state accuracy was achieved. The final PI controller parameters used throughout the simulation are listed in Table 4.

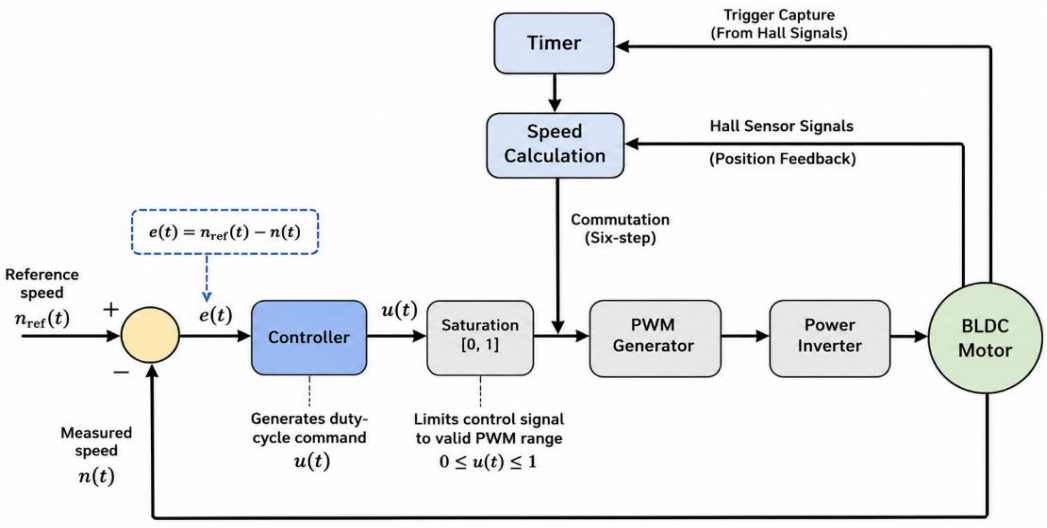

Figure 8. Closed-loop simulation model structure

2.3.3. FOPID controller design and parameter tuning

The fractional-order proportional-integral-derivative (FOPID) controller is implemented to enhance the dynamic performance of the BLDC motor speed control system by introducing two additional tuning parameters, namely the fractional integral order λ and the fractional derivative order μ. Compared with the conventional PI controller, the FOPID controller provides greater flexibility in controller design, allowing improved transient response, disturbance rejection, and robustness over a wider operating range [13], [14]. The transfer function of the FOPID controller is expressed as (11).

$$G_{FOPID}(s) = K_p + \frac{K_i}{s^{\lambda}} + K_d s^{\mu} \quad (11)$$

Where K_p, K_i, and K_d denote the proportional, integral, and derivative gains, respectively, while λ and μ represent the fractional orders of the integral and derivative terms.

Figure 10 illustrates the implementation of the FOPID controller in the proposed closed-loop speed control system. The FOPID controller was implemented using the $PI^{\lambda}D^{\mu}$ block available in the FOMCON Toolbox for MATLAB/Simulink. The fractional-order integral and derivative operators were realized using the Oustaloup recursive approximation, which approximates the fractional-order operators by equivalent rational transfer functions for numerical implementation. In this study, a fifth-order Oustaloup approximation was adopted over the frequency range of 0.1 to 500 rad/s, providing an appropriate approximation bandwidth for the dynamic behavior of the BLDC motor drive. The final controller parameters used throughout the simulation are summarized in Table 5. The controller parameters were determined through an iterative simulation-based tuning procedure under the operating conditions described in section 2.3. The controller gains K_p, K_i, and K_d together with the fractional orders λ and μ were gradually adjusted to obtain a satisfactory balance between rise time, settling time, overshoot, steady-state accuracy, and disturbance rejection.

Table 4. BLDC motor specifications

Parameter	Value
K_p	20
K_i	55

Table 5. FOPID controller parameters

Parameter	Value	Parameter	Value
K_p	20	λ	0.95
K_i	60	μ	0.8
K_d	0.01		

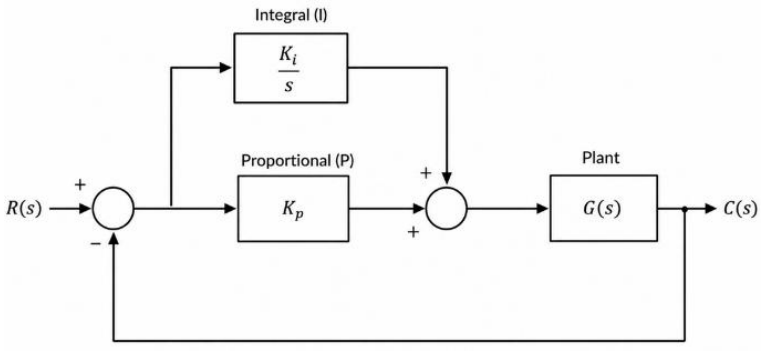

Figure 9. Block diagram of the PI controller structure

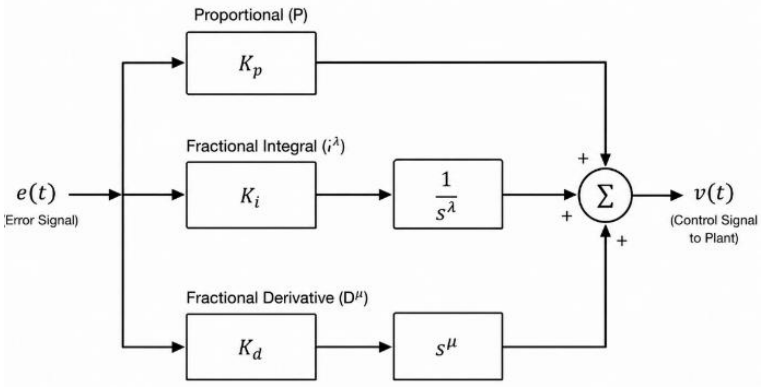

Figure 10. Block diagram of the FOPID controller structure

2.3.4. Low-pass pre-filter

A first-order low-pass pre-filter is incorporated at the reference input to improve the transient response of the proposed BLDC motor speed control system. Instead of directly applying the reference speed to the controller, the pre-filter smooths abrupt changes in the reference signal before it is processed by the PI or FOPID controller. This reduces excessive control action during step changes and helps suppress overshoot while maintaining satisfactory tracking performance. Since the pre-filter acts only on the reference signal, the controller structure and tuning parameters remain unchanged. The transfer function of the low-pass pre-filter is given by (12).

$$G_f(s) = \frac{1}{\tau_f s+1} \tag{12}$$

Where τ_f represents the filter time constant. The value of τ_f determines the degree of filtering applied to the reference signal. A shorter time constant will result in a faster response with less filtering, while a larger one will lead to better attenuation of abrupt reference changes, but it may lead to more delay and adversely affect the transient performance. Thus, a value of τ f should be sufficient to smooth the response without significantly slowing the speed control system overall.

Figure 11 shows the implementation of the proposed low-pass pre-filter in the BLDC motor speed control system. The pre-filter is positioned before the controller so that the filtered reference signal is provided to PI and FOPID controllers under the same operating conditions. This way, any improvement in the transient response is attributed to the pre-filter and not to controller parameters. The time constant was determined in a preliminary simulation and for several candidate values under the same operating conditions that we used during the present work.

The selection was based on the transient performance of the speed response, considering rise time, settling time, overshoot, and steady-state accuracy. Smaller values of τ_f provided limited smoothing of abrupt reference changes, whereas larger values introduced noticeable delays in speed tracking. Based on these

observations, a time constant of 0.015 s was selected as a suitable compromise between response speed and reference smoothing.

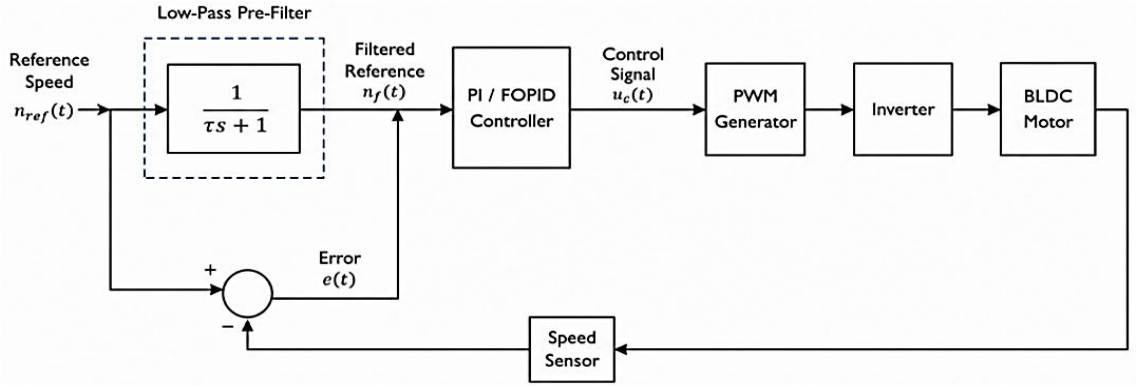

Figure 11. Block diagram of the low-pass pre-filter integrated into the proposed speed control system.

2.3. Simulation model configuration

To ensure a consistent and fair comparison between the PI and FOPID controllers, a unified simulation model was developed in the MATLAB/Simulink environment. The model consists of a BLDC motor, a three-phase inverter, Hall-effect sensor feedback, speed calculation, and a PWM generator. A manual switch was incorporated to enable the selection of either the PI or FOPID controller while maintaining the same plant model and operating conditions. Consequently, the performance differences observed during the simulations are solely attributed to the selected controller rather than variations in the simulation model. Figure 12 illustrates the original Simulink implementation used to evaluate the PI and FOPID controllers without the low-pass pre-filter. Both controllers share the same BLDC motor model, inverter, PWM generator, and feedback path, while the manual switch allows only one controller to be activated during each simulation.

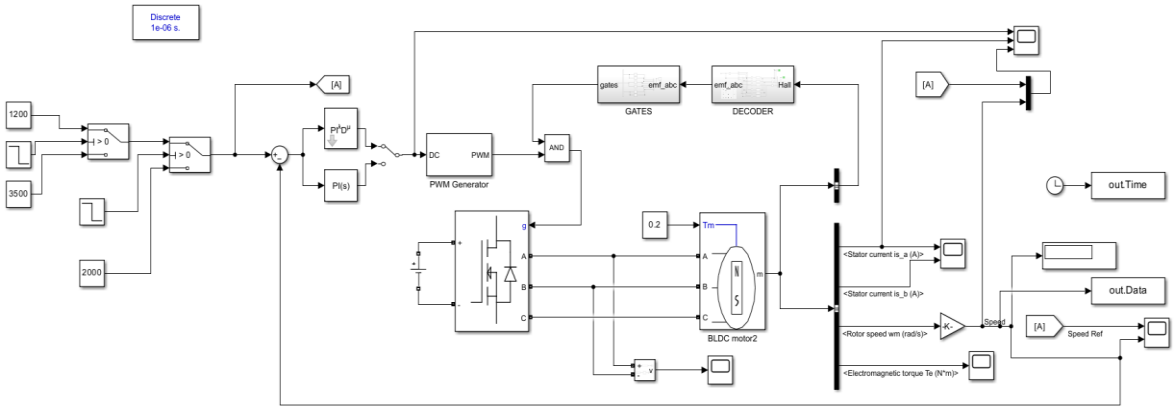

Figure 12. Simulink model for PI and FOPID controller evaluation

To investigate the influence of the reference low-pass pre-filter, the original simulation model was modified by inserting a first-order low-pass pre-filter before the error calculation block. Apart from this modification, the controller parameters, motor parameters, PWM generator, inverter model, Hall-effect sensor feedback, and operating conditions remained unchanged. This configuration enables the effect of the pre-filter to be evaluated independently without introducing additional variables into the control system.

Figure 13 shows the modified Simulink model incorporating the proposed low-pass pre-filter. Using the same simulation platform for all controller configurations ensures that the comparison between the PI controller, FOPID controller, PI with low-pass pre-filter, and FOPID with low-pass pre-filter is performed under identical operating conditions. The controller performance was evaluated using identical simulation

conditions for all controller configurations. The same reference speed profile, load torque, BLDC motor parameters, inverter configuration, and controller operating conditions were maintained throughout the study.

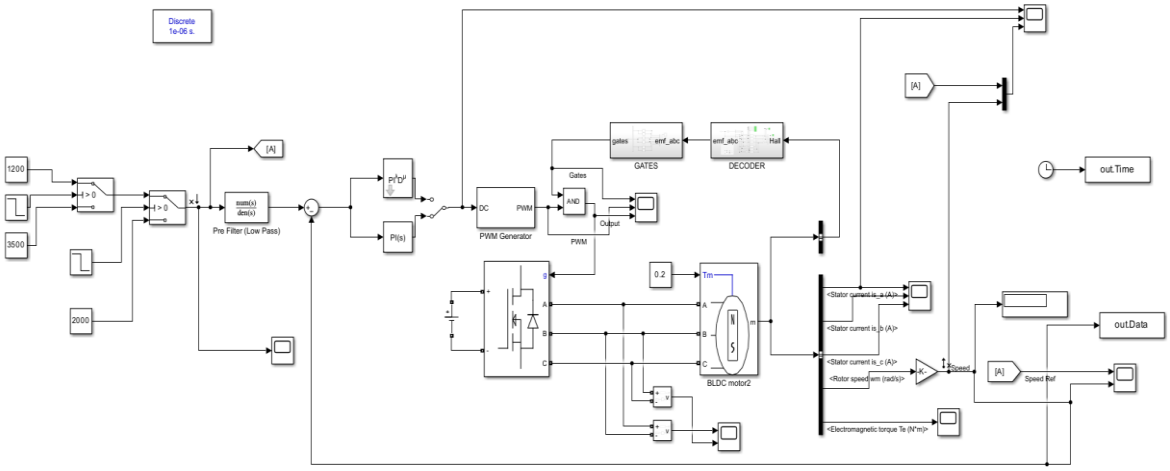

Figure 13. Simulink model with the proposed low-pass pre-filter integrated into the reference path

3. RESULTS AND DISCUSSION

This section presents the open-loop experimental results and the corresponding simulation validation, followed by the closed-loop speed control comparison using PI and FOPID controllers with and without a low-pass pre-filter. Controller performance is evaluated and discussed using time-domain indicators such as rise time, settling time, percentage overshoot, percentage undershoot, and steady-state error, to compare transient response quality and steady-state stability.

3.1. Closed-loop speed response without low-pass pre-filter

The proposed closed-loop speed control system was first evaluated without the reference low-pass pre-filter to compare the inherent performance of the conventional PI controller and the FOPID controller under identical operating conditions. Both controllers were tested using the same multi-step reference speed profile (1200–3500–2000 rpm) with a constant load-torque disturbance of 0.2 Nm. The corresponding speed responses are illustrated in Figure 14 and Figure 15, while the extracted time-domain performance indices are summarized in Table 6.



Figure 14. Simulated closed-loop speed response of the BLDC motor using a PI controller



Figure 15. Simulated closed-loop speed response of the BLDC motor using a FOPID controller

Table 6. Performance comparison between PI and FOPID

Speed transition (rpm)	Controller	Overshoot (%)	Undershoot (%)	Settling time (s)	Rise time (s)	Steady-state error (%)
0 → 1200	PI	30.49	0	0.0139	0.00347	0.5
	FOPID	30.33	0	0.139	0.004	0.417
1200 → 3500	PI	1.174	0	0.105	0.006	0.618
	FOPID	1.01	0	0.235	0.007	0.485
3500 → 2000	PI	0	0.675	0.433	0.036	0.1
	FOPID	0	4.2	0.5	0.036	0.95

Both controllers successfully tracked the reference speed throughout the simulation, indicating that the proposed closed-loop configuration provides stable operation under the selected test conditions. The PI controller generally exhibited shorter settling times, particularly during acceleration and deceleration, indicating a faster transient recovery. In contrast, the FOPID controller achieved slightly lower overshoot and improved steady-state accuracy during speed increases, although this improvement was accompanied by a longer settling time in several operating conditions.

The different transient characteristics can be attributed to the additional fractional integral and derivative orders incorporated in the FOPID controller. These additional tuning parameters provide greater flexibility in shaping the controller dynamics, allowing better regulation of the steady-state response while introducing a more gradual transient response. Consequently, the results indicate that the conventional PI controller offers faster recovery, whereas the FOPID controller provides improved tracking accuracy, demonstrating the trade-off between transient speed and steady-state performance.

3.2. Closed-loop speed response with low-pass pre-filter

To investigate the influence of reference signal conditioning, a first-order low-pass pre-filter was incorporated before the PI and FOPID controllers while maintaining the same controller parameters, BLDC motor model, inverter configuration, and operating conditions. The corresponding speed responses are presented in Figures 16 and 17, and the extracted performance indices are listed in Table 6. To evaluate the PI and FOPID controller with pre-filter response in Figures 14 and 15, the time-domain performance indices were extracted for each step change in the reference speed command (1200 rpm, 3500 rpm, and 2000 rpm). The indices include overshoot, undershoot, settling time, rise time, and steady-state error, as listed in Table 7.

The introduction of the low-pass pre-filter noticeably improved the transient characteristics of both controllers. Instead of applying abrupt step changes directly to the controller input, the reference command was gradually smoothed before entering the feedback loop. This reduced excessive controller action during rapid speed transitions, resulting in the complete elimination of overshoot for both PI and FOPID controllers across all evaluated operating conditions.

Although the pre-filter slightly moderated the initial response during some speed transitions, the resulting speed profiles became considerably smoother and more stable. Such behavior is particularly desirable for Electric Power Steering applications, where abrupt speed variations may reduce steering smoothness and driver comfort. The smoother response produced by the pre-filter therefore represents a practical improvement without requiring any modification to the controller structure itself.

Among the evaluated configurations, the FOPID controller combined with the reference low-pass pre-filter demonstrated the most balanced overall performance. It maintained smooth transient behavior while achieving shorter settling times and lower steady-state error during several operating conditions. These findings indicate that combining fractional-order control with reference signal conditioning can improve both transient quality and tracking accuracy under the simulated operating conditions.

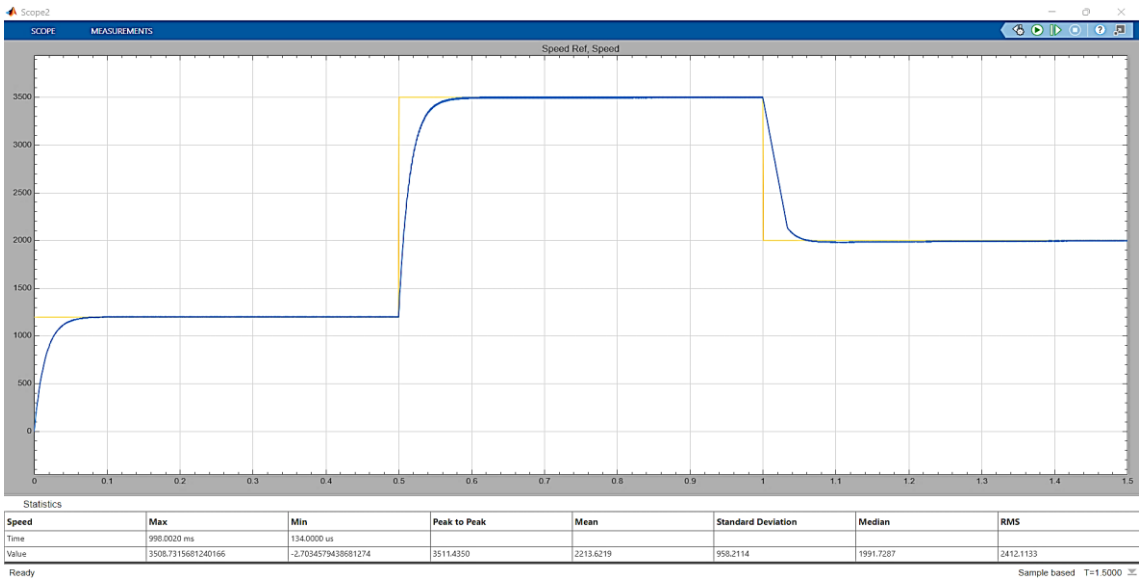

Figure 16. Simulated closed-loop speed response of the BLDC motor using a PI controller with low-pass pre-filter

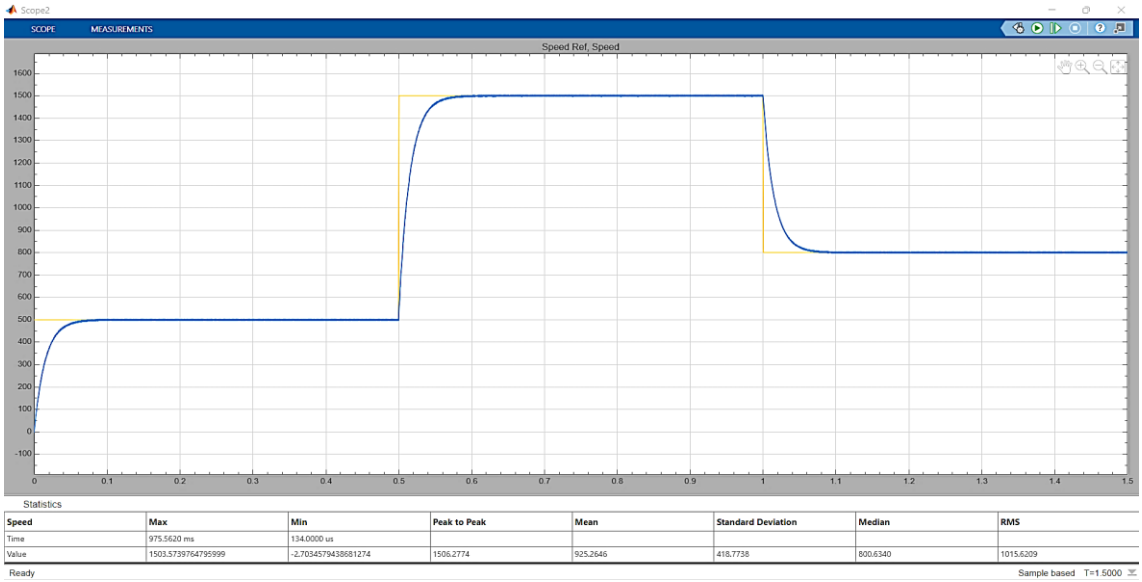

Figure 17. Simulated closed-loop speed response of the BLDC motor using a FOPID controller with low-pass pre-filter

Table 7. Performance comparison between PI and FOPID with pre-filter

Speed transition (rpm)	Controller	Overshoot (%)	Undershoot (%)	Settling time (s)	Rise time (s)	Steady-state error (%)
0 → 1200	PI	0	0	0.13	0.042	0.4
	FOPID	0	0	0.042	0.5	0.438
1200 → 3500	PI	0	0	0.14	0.034	0.49
	FOPID	0	0	0.148	0.0345	0.393
3500 → 2000	PI	0	0.523	0.272	0.04	0.146
	FOPID	0	0.515	0.045	0.0358	0.112

3.3. Discussion and limitations

The results of the present study can be viewed in a broad framework of BLDC motor control. The traditional PI controllers are widely used due to their simple implementation and tuning procedure and relatively low computational cost in industry. However, their fixed controller gains may reduce performance in extreme cases of system operating conditions and system dynamics (e.g., nonlinear behavior and external disturbances). In order to overcome these limitations, various work has been undertaken on adaptive PI, sliding mode control, model predictive control, and fractional-order controllers [12]–[14], [16].

These control strategies generally improve the system's robustness and transient performance, but tend to require more sophisticated controller structures, parameter adaptation or higher computational effort. Unlike these advanced adaptive or nonlinear control techniques, our approach improves the transient behavior by implementing a simple first-order reference low-pass pre-filter without modifying the basic controller structure. The simulation results demonstrate that this modification can effectively remove overshoot for PI and FOPID controllers while keeping the tracking speed constant. Furthermore, the FOPID controller with the pre-filter has better settling behavior and steady-state accuracy for a number of operating conditions. Thus, the proposed setup offers a compromise between improving transient performance and simplicity of implementation for future electric power steering applications where computational efficiency and controller reliability are important.

Despite these promising results, there are some limitations. The present study is based on MATLAB/Simulink simulations, and experimental validation at a real BLDC motor drive has not yet been done. Therefore, the practical effects such as sensor noise, inverter dead time, switching losses, computational delay and measurement uncertainty are not considered in this study. In addition, controller performance was evaluated with a fixed BLDC motor model under constant load-torque disturbance. The effects of parameter variations, thermal changes and wider operating conditions are not considered in this work. These limitations should be considered when interpreting the present findings and provide a motivation to further experiments and controller improvements.

4. CONCLUSION

This paper presented a closed-loop BLDC motor speed control strategy for electric power steering (EPS) applications for a FOPID controller with a reference low-pass pre-filter. A general MATLAB/Simulink model with PWM generation, inverter switching, Hall sensor commutation, and speed feedback was developed to evaluate four controller configurations for the same operating conditions: PI, FOPID, PI with low-pass pre-filter, and FOPID with low-pass pre-filter. The simulation results show that both PI and FOPID controllers can provide stable closed-loop speed regulation. Without the reference low-pass pre-filter, the PI controller generally provides faster transient recovery and the FOPID controller provides slightly better steady-state accuracy in some of the operating conditions. The reference low-pass pre-filter significantly improved the transient characteristics of both controllers, leading to no overshoot and smooth speed transitions without any changes in controller structure. In all of the cases that were analyzed, the FOPID controller with the reference low-pass pre-filter was the most balanced in terms of settling behavior, transient smoothness, and steady-state accuracy. These properties are especially beneficial for electric power steering systems where smooth motor response and correct speed regulation result in steering smoothness, driving comfort, and quality steering support in varying operating conditions. The proposed method therefore offers an innovative and practical solution for improving BLDC motor speed regulation with a relatively simple control structure for embedded applications.

Although this work is only simulation-based, the results we obtained should provide a basis for further development of BLDC motor control systems for EPS applications. Future work will focus on implementing the proposed PI and FOPID controllers with the reference low-pass pre-filter on the embedded real-time platform and test them on a laboratory BLDC motor drive. Further studies will be conducted to understand the performance of the controller under parameter changes, measurement noise, steering loads, and realistic driving situations to determine how robust it is for practical EPS applications. It will also be studied for systematic optimization techniques to further improve controller performance while maintaining the computational efficiency required for applications in automotive embedded systems.

ACKNOWLEDGEMENT

The authors wish to express their gratitude to the Universiti Teknikal Malaysia Melaka (UTeM), Fakulti Teknologi dan Kejuruteraan Elektrik (FTKE), Centre of Robotic and Industrial Automation (CERIA) and Centre of Research and Innovation Management (CRIM).

FUNDING INFORMATION

This research was financially supported by the Centre of Research and Innovation Management (CRIM), Universiti Teknikal Malaysia Melaka (UTeM), which covered the article processing fee.

AUTHOR CONTRIBUTIONS STATEMENT

This journal uses the Contributor Roles Taxonomy (CRediT) to recognize individual author contributions, reduce authorship disputes, and facilitate collaboration.

Name of Author	C	M	So	Va	Fo	I	R	D	O	E	Vi	Su	P	Fu
Amir Haziq Nordin	✓	✓	✓	✓	✓	✓		✓	✓	✓			✓	
Azrita Alias			✓		✓	✓		✓	✓	✓	✓	✓		
Auzani Jidin	✓	✓		✓	✓				✓		✓	✓		
Maaspaliza Azri		✓		✓	✓					✓	✓			
Tole Sutikno		✓		✓	✓					✓	✓			

C : **C**onceptualization
M : **M**ethodology
So : **So**ftware
Va : **Va**lidation
Fo : **Fo**rmal analysis
I : **I**nvestigation
R : **R**esources
D : **D**ata Curation
O : Writing - **O**riginal Draft
E : Writing - Review & **E**diting
Vi : **Vi**sualization
Su : **Su**pervision
P : **P**roject administration
Fu : **Fu**nding acquisition

CONFLICT OF INTEREST STATEMENT

The authors declare that they have no known competing financial interests or personal relationships that could have appeared to influence the work reported in this paper. Authors state no conflict of interest.

DATA AVAILABILITY

Data availability is not applicable to this paper as no new data were created or analyzed in this study.

REFERENCES

[1] M. B. Baharom, K. Hussain, and A. J. Day, "Design of full electric power steering with enhanced performance over that of hydraulic power-assisted steering," *Proceedings of the Institution of Mechanical Engineers, Part D: Journal of Automobile Engineering*, vol. 227, no. 3, pp. 390–399, Mar. 2013, doi: 10.1177/0954407012468413.

[2] Somashekarappa M and Rajesh S R, "Electric power steering systems: Electronic control strategies for enhanced performance and efficiency," *World Journal of Advanced Research and Reviews*, vol. 12, no. 2, pp. 668–679, Nov. 2021, doi: 10.30574/wjarr.2021.12.2.0492.

[3] M. Sharma, S. Sharma, and J. Vajpai, "Controlling methods of brushless DC motor in electrical vehicle drives," in *Lecture Notes in Electrical Engineering*, 2024, pp. 717–726, doi: 10.1007/978-981-99-6749-0_46.

[4] S. P. Singh, K. K. Singh, K. S. Verma, J. Singh, and N. Tiwari, "A review on control of a brushless DC motor drive," *International Journal on Future Revolution in Computer Science & Communication Engineering*, vol. 4, no. 1, pp. 82–97, 2018.

[5] M. Soora, A. Vandhana, and V. Srujana, "Torque ripple minimization of a BLDC motor drive by using electronic commutation and speed, current controllers," *International journal of Engineering, Business and Management (IJEBM)*, vol. 1, no. 1, pp. 19–27, 2017.

[6] J.-H. Song and I. Choy, "Commutation torque ripple reduction in brushless DC motor drives using a single DC current sensor," *IEEE Transactions on Power Electronics*, vol. 19, no. 2, pp. 312–319, Mar. 2004, doi: 10.1109/TPEL.2003.823177.

[7] N. Prabhu, R. Thirumalaivasan, and B. Ashok, "Critical review on torque ripple sources and mitigation control strategies of BLDC motors in electric vehicle applications," *IEEE Access*, vol. 11, pp. 115699–115739, 2023, doi: 10.1109/ACCESS.2023.3324419.

[8] M. S. Zaky, "A self-tuning PI controller for the speed control of electrical motor drives," *Electric Power Systems Research*, vol. 119, pp. 293–303, Feb. 2015, doi: 10.1016/j.epsr.2014.10.004.

[9] M. W. Foley, N. R. Ramharack, and B. R. Copeland, "Comparison of PI controller tuning methods," *Industrial & Engineering Chemistry Research*, vol. 44, no. 17, pp. 6741–6750, Aug. 2005, doi: 10.1021/ie040258o.

[10] M. Mahmud, M. R. Islam, S. M. A. Motakabber, M. D. A. Satter, K. E. Afroz, and A. K. M. Ahasan Habib, "Control speed of BLDC motor using PID," in *2022 IEEE 18th International Colloquium on Signal Processing & Applications (CSPA)*, IEEE, May 2022, pp. 150–154, doi: 10.1109/CSPA55076.2022.9782030.

[11] A. Azwin and S. Ahmed, "Induction motor speed control using varied duty cycle terminal voltage via PI controller," *IOP Conference Series: Materials Science and Engineering*, vol. 341, Mar. 2018, doi: 10.1088/1757-899X/341/1/012013.
[12] P. Damodharan and K. Vasudevan, "Sensorless brushless DC motor drive based on the zero-crossing detection of back electromotive force (EMF) From the line voltage difference," *IEEE Transactions on Energy Conversion*, vol. 25, no. 3, pp. 661–668, Sep. 2010, doi: 10.1109/TEC.2010.2041781.
[13] S. A. S. A. Zawawi, A. Jidin, N. S. M. Sabri, S. A. A. Tarusan, and T. Sutikno, "Enhanced torque control in high-speed DTC using modified stator flux locus," *International Journal of Power Electronics and Drive Systems (IJPEDS)*, vol. 16, no. 1, pp. 457-463, Mar. 2025, doi: 10.11591/ijpeds.v16.i1.pp457-463.
[14] W. S. H. Wong and D. Holliday, "Minimisation of flux droop in direct torque controlled induction motor drives," *IEE Proceedings - Electric Power Applications*, vol. 151, no. 6, pp. 694–703, Nov. 2004, doi: 10.1049/ip-epa:20040681.
[15] R. El-Khazali, "Fractional-order ???×?? controller design," *Computers & Mathematics with Applications*, vol. 66, no. 5, pp. 639–646, Sep. 2013, doi: 10.1016/j.camwa.2013.02.015.
[16] M. Sharma, S. Sharma, and J. Vajpai, "A novel approach to design and analyze fractional order PID controller for speed control of brushless DC motor," *Renewable Energy and Sustainable Development*, vol. 10, no. 2, Sep. 2024, doi: 10.21622/resd.2024.10.2.903.
[17] M. A. George, D. V. Kamat, and T. Indiran, "OTA-C realization of an optimized FOPID controller for BLDC motor speed control," *IETE Journal of Research*, vol. 69, no. 1, pp. 118–136, Jan. 2023, doi: 10.1080/03772063.2021.1951380.
[18] W. A. Salah, D. Ishak, K. J. Hammadi, and S. Taib, "Development of a BLDC motor drive with improved output characteristics," *Przegląd Elektrotechniczny (Electrical Review)*, vol. 87, no. 3, pp. 258–261, 2011.
[19] S. Balaji and M. Venkatesan, "BLDC motor control based on duty cycle," in *2017 IEEE International Conference on Computational Intelligence and Computing Research (ICCIC)*, IEEE, Dec. 2017, pp. 1–4, doi: 10.1109/ICCIC.2017.8524307.
[20] Chin-Long Wey, Chung-Hsien Hsu, and Tai-Wei Chang, "A voltage-mode boost DC-DC converter with a constant-duty-cycle pulse control," in *2013 IEEE 4th Latin American Symposium on Circuits and Systems (LASCAS)*, IEEE, Feb. 2013, pp. 1–4, doi: 10.1109/LASCAS.2013.6518983.
[21] H.-C. Wu, M.-Y. Wen, and C.-C. Wong, "Speed control of BLDC motors using Hall effect sensors based on DSP," in *2016 International Conference on System Science and Engineering (ICSSE)*, IEEE, Jul. 2016, pp. 1–4, doi: 10.1109/ICSSE.2016.7551633.
[22] R. Ristiana *et al.*, "Novel hybrid-MPCC approach to generate switching sequence for six-step commutation of BLDC motor using Hall effect sensor," *Alexandria Engineering Journal*, vol. 82, pp. 43–54, Nov. 2023, doi: 10.1016/j.aej.2023.09.052.
[23] P. Damodharan, R. Sandeep, and K. Vasudevan, "Simple position sensorless starting method for brushless DC motor," *IET Electric Power Applications*, vol. 2, no. 1, pp. 49–55, Jan. 2008, doi: 10.1049/iet-epa:20070229.
[24] G. Prasad, N. S. Ramya, P. V. N. Prasad, and G. T. R. Das, "Modelling and simulation analysis of the brushless DC motor by using MATLAB," *International Journal of Innovative Technology and Exploring Engineering (IJITEE)*, vol. 1, no. 5, pp. 27–31, 2012.
[25] T.-U. Jung, J.-H. Jang, and C.-S. Park, "A back-EMF estimation error compensation method for accurate rotor position estimation of surface mounted permanent magnet synchronous motors," *Energies*, vol. 10, no. 8, Aug. 2017, doi: 10.3390/en10081160.
[26] J. C. Gamazo-Real, E. Vázquez-Sánchez, and J. Gómez-Gil, "Position and speed control of brushless DC motors using sensorless techniques and application trends," *Sensors*, vol. 10, no. 7, pp. 6901–6947, Jul. 2010, doi: 10.3390/s100706901.
[27] N.-A. Truong, H.-L. Thai, and T.-G. Nguyen, "Dedicated SoC peripheral design for power control applications on the Xilinx Ultrascale+ Platform," *Journal of Technical Education Science*, Oct. 2025, doi: 10.54644/jte.2025.1881.
[28] G. Elhassan *et al.*, "Investigation on multisampling deadbeat current control with time-delay compensation in grid-connected inverter," *IEEE Access*, vol. 11, pp. 12444–12459, 2023, doi: 10.1109/ACCESS.2023.3239662.

BIOGRAPHIES OF AUTHORS



Amir Haziq bin Nordin was born in Malaysia in 2001. He received his bachelor's degree in electrical engineering from Universiti Teknikal Malaysia Melaka (UTeM), Malaysia, in 2026. He is currently pursuing a Master of Engineering (M.Eng.) degree. His research interests include motor modelling, control systems, power electronics, electric drive systems, and simulation studies. He can be contacted at email: amirhaziq015@gmail.com.



Azrita binti Alias received her Bachelor of Engineering (B.Eng.) degree with Honours in electrical engineering (control and instrumentation) and her Master of Engineering (M.Eng.) degree in electrical engineering from Universiti Teknologi Malaysia (UTM) in 2000 and 2003, respectively. She received her Doctor of Philosophy (Ph.D.) degree from the University of Malaya in 2015. She is currently a senior lecturer at the Faculty of Electrical Technology and Engineering, Universiti Teknikal Malaysia Melaka (UTeM), Malaysia. She is also an active researcher with the EV-Prodrives Research Group and serves as the head of the Bachelor of Electrical Engineering with Honours (Part-Time) (BELG) programme at UTeM. Her research interests include modelling, control system analysis, power electronics, motor drive systems, and engineering applications. She can be contacted at email: azrita@utem.edu.my.



Auzani bin Jidin received his Bachelor of Engineering (B.Eng.), Master of Engineering (M.Eng.), and Doctor of Philosophy (Ph.D.) degrees in power electronics and drives from Universiti Teknologi Malaysia (UTM), Johor Bahru, Malaysia, in 2002, 2004, and 2011, respectively. He is currently a senior lecturer at the Faculty of Electrical Technology and Engineering, Universiti Teknikal Malaysia Melaka (UTeM), Malaysia. He is also an active researcher with the EV-Prodrives Research Group, focusing on power electronics and drives (PED), electric machine design (EMD), and electric vehicle drives (EVD). His research interests include power electronics, electric motor drive systems, field-programmable gate arrays (FPGAs), digital signal processors (DSPs), and electric vehicle drive technologies. He can be contacted at email: auzani@utem.edu.my.



Maaspaliza binti Azri received her Bachelor of Engineering (B.Eng.) degree with Honours in electrical engineering from Universiti Teknologi MARA in 2001 and her Master of Science (M.Sc.) degree in electrical power engineering from Universiti Putra Malaysia in 2004. She received her Ph.D. degree from the University of Malaya Power Energy Dedicated Advanced Centre (UMPEDAC), University of Malaya, in 2014. Since 2015, she has been a senior lecturer at the Faculty of Electrical Technology and Engineering, Universiti Teknikal Malaysia Melaka (UTeM). She also served as the head of the Department of Electrical Engineering from 2018 to 2020. She has been a Chartered Engineer registered with the Institution of Engineering and Technology (IET), United Kingdom, and a Professional Engineer registered with the Board of Engineers Malaysia (BEM) since 2023. Her research interests include power electronics and renewable energy. She can be contacted at email: maaspaliza@utem.edu.my.



Prof. Ir. Tole Sutikno, S.T., M.T., Ph.D., MIET, IPM., ASEAN Eng. is a lecturer and the head of the Master Program of Electrical Engineering at the Faculty of Industrial Technology, Universitas Ahmad Dahlan (UAD) in Yogyakarta, Indonesia. In addition to leading the master program, he also lectures in the Ph.D. program in informatics and the undergraduate program in electrical engineering at UAD. He received his Bachelor of Engineering from Universitas Diponegoro in 1999, Master of Engineering from Universitas Gadjah Mada in 2004, and Doctor of Philosophy in Electrical Engineering from Universiti Teknologi Malaysia in 2016. All three degrees are in the electrical engineering area. He has been a professor at UAD in Yogyakarta, Indonesia, since July 2023, following his tenure as an associate professor in June 2008. He is the Editor-in-Chief of TELKOMNIKA and Head of the Embedded Systems and Power Electronics Research Group (ESPERG). He is listed as one of the top 2% of researchers worldwide, according to Stanford University and Elsevier BV's list of the most influential scientists from 2021 to the present. His research interests cover digital design, industrial applications, industrial electronics, industrial informatics, power electronics, motor drives, renewable energy, FPGA applications, embedded systems, artificial intelligence, intelligent control, digital libraries, and information technology. He can be contacted at email: tole@te.uad.ac.id or thsutikno@ieee.org.